ACI STRUCTURAL JOURNAL TECHNICAL PAPER
Title no. 90-S44

Confined Concrete Columns with Stubs

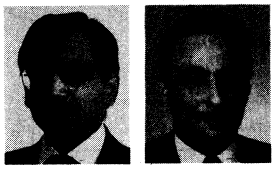

by Shamim A. Sheikh and Shafik S. Khoury

The critical sections of columns in a framed structure subjected to earthquake loads are invariably adjacent to the beam-column/slab joints or the footings. External restraint provided by the heavy elements alters the behavior of the adjacent sections and may not always prove conservative. To simulate this behavior, six reinforced concrete columns, 12 x 12 x 58 in. (305 x 305 x 1473 mm), each cast integrally with a 20 x 30 x 32-in. (508 x 762 x 813-mm) stub, were tested under cyclic flexure and shear while simultaneously subjected to a constant axial load. The variables in the test program were the amount of lateral steel, steel configuration, and level of axial load. From a comparison of the results from this test series with those from similar prismatic specimens tested earlier, it was concluded that the stub enhanced the adjacent section's flexural strength by more than 20 percent. Increase in the amount of lateral steel, reduction in axial load, and increased effectiveness of the lateral support provided to the longitudinal bars result in an increase in ductility and energy-absorbing capacity of the columns. The maximum usable compressive strain for confined concrete was found to be in the range of 0.025 to 0.042, and the equivalent plastic hinge length was approximately equal to the section size, irrespective of the variables examined.

Keywords: axial loads; columns (supports); confined concrete; elasto-plastic behavior; earthquakes; energy absorption; **hinges (structural).**

Although it is preferable to design a structure such that it behaves in an elastic mode without suffering much damage during an extreme event, economic realities dictate a different design approach. Allowing inelastic deformations in flexural members during a severe earthquake is a common and preferred technique to dissipate seismic energy. However, with the uncertainties of loading and the overall structural behavior, it is difficult to avoid inelastic actions in columns. In the members whose behavior is dominated by axial compression, brittle failure as a result of inelastic deformation can be avoided only if the concrete is made to behave in a ductile manner with the help of confinement provided by lateral and longitudinal steel, and if the longitudinal reinforcement is restrained adequately against premature buckling.

Work presented here is part of an ongoing research program in which the behavior of reinforced concrete columns is studied under a variety of loading conditions with the aim of establishing guidelines for the design and detailing of confining steel for a certain performance of the section and the member. In the initial stages, columns with different steel arrangements were tested under monotonic concentric compression, and an analytical model for the mechanism of confinement was developed.[1,2] Most recent work has dealt with columns under axial load and flexure.[3] All of this work involved prismatic members. The current phase of the study deals with nonprismatic specimens in which the critical section of the column is adjacent to a heavy stub that represents an undamaged beam-column joint area or the footing. It is believed that the external restraint provided by the stub alters the member behavior in a way that may not always be conservative. The columns were subjected to cyclic shear and flexure while being subjected to a constant axial load throughout the test.

RESEARCH SIGNIFICANCE

The current North American design code[4,5] requirements do not consider steel detailing, type of load, or performance of columns in the design of confinement steel. If a column designed according to those code requirements performs satisfactorily for a certain combination of geometric and load conditions, it may be unsafe for more severe conditions, such as higher ductility demand or higher axial load. For less severe conditions or less ductile performance requirements, the design according to those codes would be unnecessarily conservative. The overall objective of this research program is to relate such design parameters as the distribution of steel, load combinations, amount of lateral steel, spacing of ties, and presence of external restraints to the performance of members, including ductility, energy absorption, and length of plastic hinge. A rational procedure and design guidelines for the design of confining steel can then be established.

EXPERIMENTAL PROGRAM

The test program consisted of six normal concrete specimens tested under cyclic lateral load while simultaneously subjected to constant axial load. The level of axial load, represented by $P/f_c'A_g$, varied between 0.47 and 0.77. Relatively high axial loads are used in this test program, considering that

ACI Structural Journal, V. 90, No. 4, July-August 1993.
Received June 18, 1992, and reviewed under Institute publication policies.

ACI member ***Shamim A. Sheikh*** *is Professor of Civil Engineering at the University of Toronto. He is a member of joint ACI-ASCE Committees 441, Reinforced Concrete Columns; and 442, Response of Concrete Buildings to Lateral Forces. His research interests include confinement of concrete, earthquake resistance of reinforced concrete, and expansive cement and its application to deep foundations.*

Shafik S. Khoury *is Assistant Professor in the Department of Structural Engineering at Alexandria University, Egypt. He received his PhD from the University of Houston in 1991. His research activities are in the area of concrete materials and reinforced concrete columns.*

various design codes[4-6] do allow high axial loads and that beneficial effects of confinement are more relevant at such axial load levels. Fig. 1 shows a sketch of the test setup.

Specimens

Each specimen consisted of a 12 x 12 x 58-in. (305 x 305 x 1473-mm) column cast integrally with a 20 x 30 x 32-in. (508 x 762 x 813-mm) stub. The core size measured from the center of the perimeter tie was kept constant at 10.5 x 10.5 in. (267 x 267 mm) for all the specimens, giving a core area equal to 77 percent of the gross area of the column. Table 1 lists details of the columns. All the columns contained eight No. 6 Grade 60 (414 MPa) longitudinal bars, providing a reinforcement ratio of 2.44 percent of the gross column cross-sectional area.

The specimens were constructed within the following tolerance of nominal dimensions: (1) overall concrete dimensions of the section = ± 1/8 in. (3 mm); (2) tie dimensions in the test region = ± 1/16 in. (1.6 mm); (3) placement of longitudinal steel = ± 1/8 in. (3 mm); and (4) spacing of ties = ± 1/8 in. (3 mm).

Steel

Eight No. 6 Grade 60 deformed bars were used in all the specimens. Lateral steel consisted of No. 3, No. 4, and 6-mm deformed bars of Grade 60 steel. Stress-strain curves of steel in tension are given in Fig. 2. Each curve represents an average of three test results. Only those parts of the curves that were needed for the analytical work for the specimens are shown. Important properties of steel are also listed on the figure. ε_y, ε_{sh}, and ε_u represent strain values at yield, at the start of strain hardening, and at rupture, respectively; f_y and f_u are the yield stress and ultimate stress, respectively. An extensometer with 2-in. (51-mm) gage length was used for all tests.

Table 1 — Specimen details and some results

Specimen	Concrete strength f'_c, ksi	Lateral steel: Size no.	Spacing, in.	Ratio ρ_s, percent	f_{yh}, ksi	$\frac{A_{sh}}{A_{sh(ACI)}}$	Axial load level: $\frac{P}{f'_c A_g}$	$\frac{P}{P_o}$	Moment: M_{smax}, k-in.	M_{max}, k-in.	M_i, k-in.	Ductility factors: μ_Δ, $0.8P_{tmax}$	μ_ϕ, $0.8M_{max}$	μ_ϕ, $0.9M_{max}$	Ductility ratios: $N_{\Delta 80}$	$N_{\Delta t}$	$N_{\phi 80}$	$N_{\phi t}$	Energy indicators: W_{80}	W_t	E_{80}	E_t
FS-9	4.70	#3	3.75	1.68	73.6	1.46	0.76	0.63	1542	1391	1131	3.1	8.0	7.5	15	21	37	44	32	44	154	163
ES-13	4.72	#4	4.50	1.69	67.3	1.34	0.76	0.63	1576	1445	1127	2.0	6.0	2.5	7	10	15	26	9	14	53	110
AS-3	4.81	#3	4.25	1.68	73.6	1.43	0.60	0.50	1806	1707	1371	4.7	19.0†	19.0†	23	32	63	74	84	127	610	753
AS-17	4.54	#3	4.25	1.68	73.6	1.52	0.77	0.63	1728	1594	1111	3.8	12.0	10.5	24	30	52	58	58	76	402	443
AS-18	4.75	#4	4.25	3.06	67.3	2.41	0.77	0.63	1892	1805	1112	6.7	17.5	14.5	44	53	80	92	263	290	897	1156
AS-19	4.68	#3, 6 mm*	4.25	1.30	73.6 67.0	1.12	0.47	0.39	1944	1789	1475	4.0	19.0	10.0	18	44	85	129	83	130	631	1230

*#3 and 6-mm bars were used for the perimeter ties and inner ties, respectively.
†The moment did not drop to $0.9M_{max}$ on the descending part of the curve.

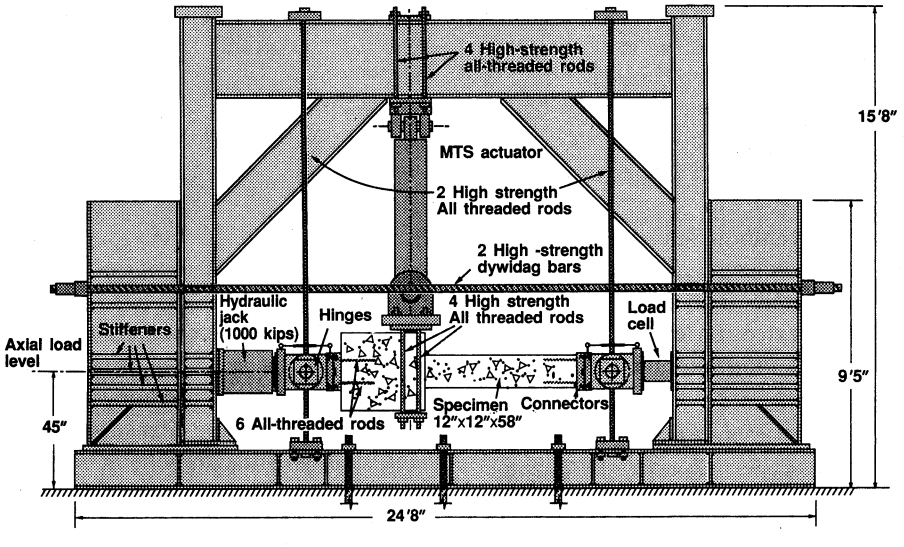

Fig. 1—Schematic test setup

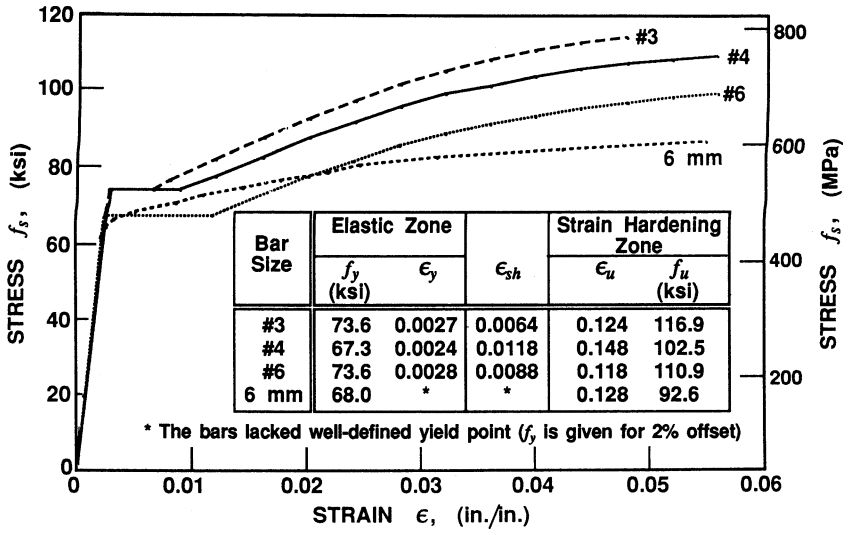

Bar Size	Elastic Zone f_y (ksi)	Elastic Zone ϵ_y	ϵ_{sh}	Strain Hardening Zone ϵ_u	Strain Hardening Zone f_u (ksi)
#3	73.6	0.0027	0.0064	0.124	116.9
#4	67.3	0.0024	0.0118	0.148	102.5
#6	73.6	0.0028	0.0088	0.118	110.9
6 mm	68.0	*	*	0.128	92.6

Fig. 2—Stress-strain behavior of steel

Concrete

Ready-mix normal weight concrete with a slump of 4 to 6 in. (102 to 152 mm) was used to cast three specimens at a time. Ordinary portland cement (ASTM Type I), natural sand, and round gravel of $^3/_8$-in. (9.5-mm) nominal maximum size were used for the mix, designed for a target strength of 4000 psi (27.6 MPa). All the specimens were cast horizontally. Strength-age relationships for the concrete from both batches were developed based on the results of 6 x 12-in. (152 x 305-mm) standard cylinders tested under compression at frequent intervals after casting. These relationships were used to calculate the strength f_c' for each specimen.

Reinforcing cages

The reinforcing cage for each specimen consisted of two parts, one for the columns and the other for the stub. The column longitudinal bars extended through the stub to $^3/_4$ in. (19 mm) from the end in all the specimens. The ties were placed at specified spacing within the test region, approximately 36 in. (914 mm) from the stub face. Outside the test region, tie spacing was reduced to minimize the chances of failure there. The reinforcement in the stub consisted of No. 4 vertical and horizontal stirrups at about 3.0-in. (76-mm) spacing. Three different steel configurations (Fig. 3) were used for the test region adjacent to the stub where most of the damage was expected.

Minimum anchorage of ties conformed to ACI Building Code requirements.[4] An extension length of at least 8 d_b (d_b = diameter of tie bar) was used for 90-deg hooks, and for 135- and 180-deg bends at least 10 d_b extension lengths were used. In many instances, $2^1/_2$-in. (63.5-mm) minimum extension length controlled the design.

Instrumentation

Extensive instrumentation was used to collect the data during each test, which included concrete and steel strain at different locations, deflection along the specimen length, and axial and lateral loads. Longitudinal steel strains along the depth on both sides of the specimen were measured by electrical resistance strain gages. Tie strains were also measured by strain gages that were laid on each leg of each tie in two selected sets within the test zone. Longitudinal concrete strains in the core were measured by using linear variable differential transformers (LVDTs) over gage lengths that varied from 2.0 to 7.0 in. (51 to 102 mm) and covered a length of about 15 in. (381 mm) from the stub-column interface. The LVDTs were mounted on $^5/_{16}$-in. (8-mm) diameter all-threaded rods that were embedded in concrete through the sections so that they did not touch longitudinal steel. About 40 strain gages and 17 LVDTs were used in each test. Fig. 3 shows the locations of the strain gages on both longitudinal and lateral steel, and a typical view of the LVDT arrangement within the test region.

TESTING

All the specimens were tested under cyclic lateral load to large inelastic deformations while being simultaneously subjected to constant axial loads. The lateral load was applied at the stub (Fig. 1) such that the most critical region of the column was adjacent to the stub and was subjected to flexure and shear in addition to axial load.

Test setup and procedure

A 12-in. (305-mm) square, 2.5-in. (63.5-mm) thick steel plate was attached to each end of the specimen using the six all-threaded $^5/_8$-in. (15.9-mm) rods embedded in the specimen end. A thin layer of plaster of paris was used between the concrete and plates to provide even surfaces. With the oversize holes in the plates, there was enough flexibility to insure that the plates and the specimen were aligned appropriately. The specimen was then placed horizontally in the loading frame and the end plates were connected to the hinges in the frame using six high-strength bolts at each end. Each hinge consisted of two units, one having two 500-kip (2224-kN) capacity bearings and the other having three similar bearings. The two units were connected with a 5.5-in. (140-mm) diameter steel shaft, the central axis of which coincided with the axis of rotation of the hinge. The specimen was supported

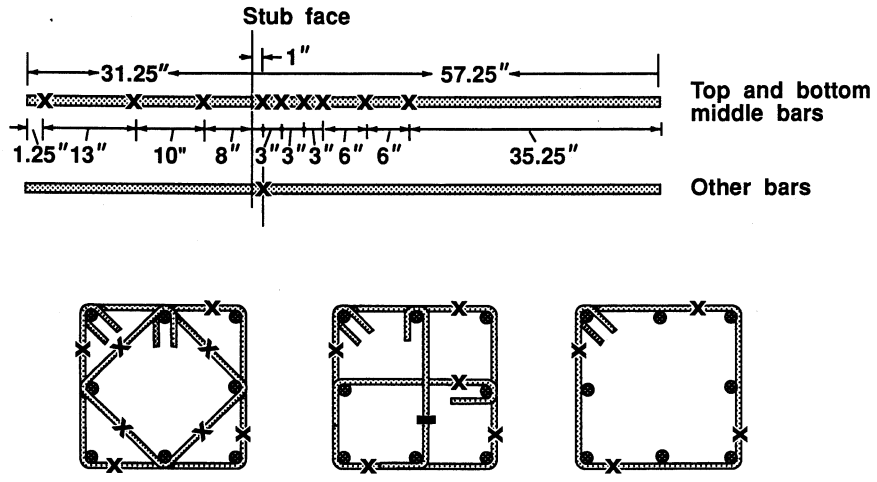

(a) Locations of strain gages on longitudinal bars and two sets of ties in test regions of columns

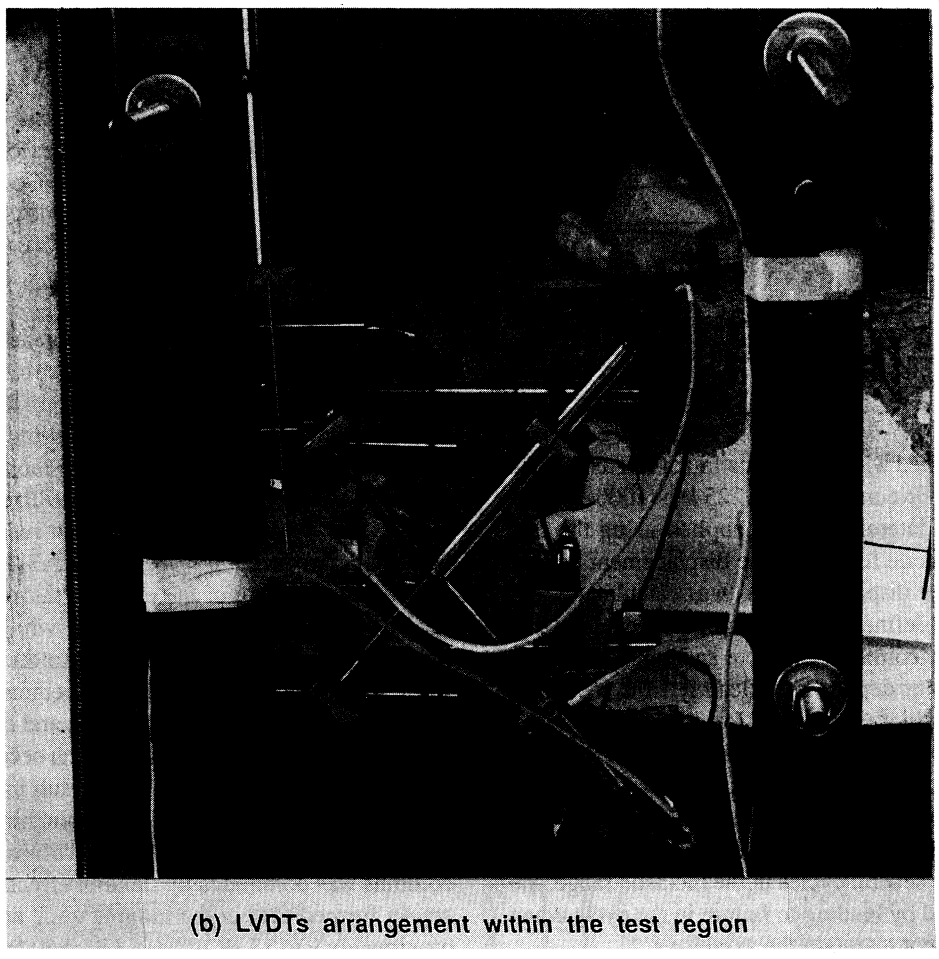

(b) LVDTs arrangement within the test region

Fig. 3—Location of strain gages and LVDTs

with the help of these shafts and connected to the top and bottom beams of the test frame (Fig. 1).

A 1000-kip (4450-kN) hydraulic jack and a similar capacity load cell were used to apply axial load. To check alignment of the specimen, axial load was applied in 50-kip (222-kN) intervals and the strain gages and LVDTs were monitored regularly. The specimen was unloaded and adjustments were made as needed. The alignment was checked up to the maximum predetermined axial load and, after the specimen was finally positioned, the load was reduced to about 1 to 2 kips (4.5 to 9 kN) and all the instrument readings were reinitialized.

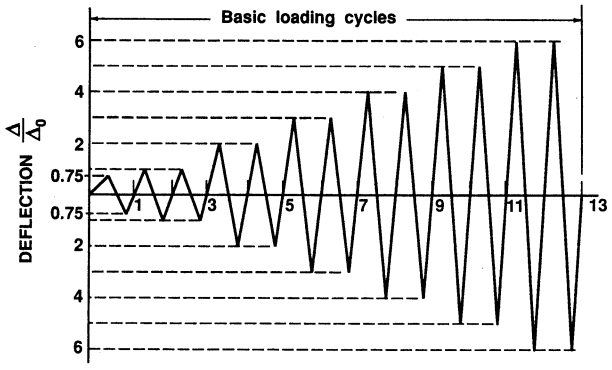

Fig. 4—Specified displacement history

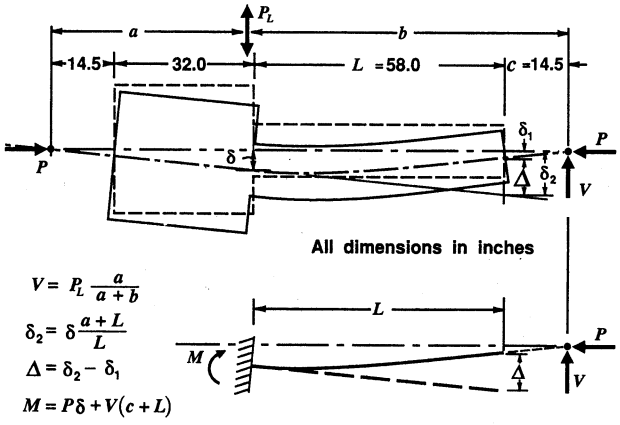

Fig. 5—Idealization of specimen

The actual test started with the application of full axial load. The specimen was then connected to a 225-kip (1000-kN) actuator (Fig. 1). The lateral load was applied using the displacement control mode following the displacement history shown in Fig. 4. The displacement Δ_o was calculated theoretically and may be defined as the yield or elastic lateral displacement for the unconfined concrete specimen, at which the specimen behavior departs significantly from a straight line. About 8 to 12 min were required to complete one cycle. The loading was stopped or slowed to a very low rate at selected points to record data, mark cracks, and take photographs. Three X-Y plotters were used to trace continuous plots of load-versus-displacements and deformations at various locations. After several cycles in the inelastic range, the tests were terminated by loading to failure in the cycle when the specimen could not maintain the axial load.

TEST RESULTS

Details of the test results are available elsewhere.[7] Here the results are presented graphically in the form of lateral load-displacement and moment-curvature relationships. Each specimen represented a portion of a column in a multistory frame between the section of maximum moment and the point of contraflexure, and was subjected to lateral load V, as shown in Fig. 5. The values of the lateral load V and lateral displacement Δ at the free end were calculated from the measured lateral applied point load P_L and the lateral displacement δ at the stub column interface. The moment M consists of two parts: the primary moment caused by the lateral load and the secondary moment caused by the axial load.

In all the specimens, the failure did not occur at the stub-column interface, although the interface was subjected to the maximum moment. The most damaged regions were shifted away from the interface because of the additional confinement provided by the stub to the adjacent concrete. The deflection at the failed section Δ_f was calculated from the deflected shape of the column, and was used to calculate the moment at that section. The curvature ϕ was calculated from the deformation readings measured by upper and lower LVDTs located at the most damaged region within the hinging zone. For comparative purposes, a constant gage length was maintained in all the specimens so far as possible, which, due to practical consideration, varied from 7.3 to 9.7 in. (185 to 246 mm). Fig. 6 through 11 show the V-Δ and M-ϕ relationships for the failed sections of all the specimens. Important events during testing such as spalling of the concrete cover, opening of the 90-deg hooks, yielding of ties, buckling of longitudinal bars, and dropping of axial load are marked on the graphs. The theoretical section moment capacity M_i and the corresponding lateral load capacity V_i are also shown on the figures. The moment capacity M_i is calculated for the unconfined section using ACI Building Code[4] specifications. The lateral load V_i is the load that will produce M_i at the critical section without considering the P-Δ effect.

Test observations

The appearance of cracks in the top and bottom concrete cover was always the first sign of distress in the test specimens. The minimum compressive strain at the extreme concrete fiber corresponding to cover crushing was about 0.0045. The first visible crushing occurred in most of the specimens during the third or fourth cycle when the applied displacement δ was being increased to about twice the elastic displacement Δ_o, except for Specimens AS-18 and AS-19. The delay in the spalling of the cover to the sixth cycle was observed clearly in Specimen AS-19, which had a relatively lightly confined section compared to the other specimens. The closely spaced lateral steel in Specimen AS-18 caused a plane of weakness between the core and cover, and resulted in an early crushing of the cover, which occurred in the second cycle. No cracking was seen in the stub in any specimen.

As seen in Fig. 6 through 11, no pinching of the loops occurred in any of the specimens. Failure mode for all the columns was dominated by flexural effects. Vertical flexural cracks formed first in the hinging zone at a distance of approximately 9 to 13 in. (229 to 330 mm) from the face of the stub, and later extended toward the stub. The most extensive damage concentrated at about 6 to 9 in. (152 to 229 mm) away from the stub face. However, spalling of the cover extended for a distance of about 15 to 30 in. (381 to 762 mm) from close to the stub. With the increase in the applied displacement, the cracks propagated further and caused successive stiffness degradations, followed by yielding of the lateral steel, and ultimately buckling of the longitudinal bars.

Extensive buckling of longitudinal bars in most cases occurred during the last cycle of loading and indicated the com-

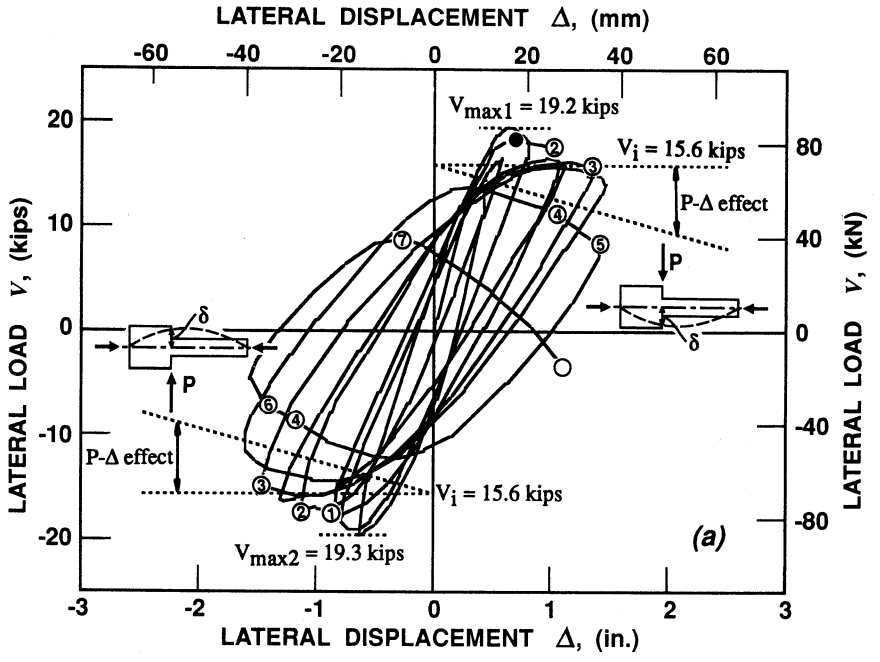

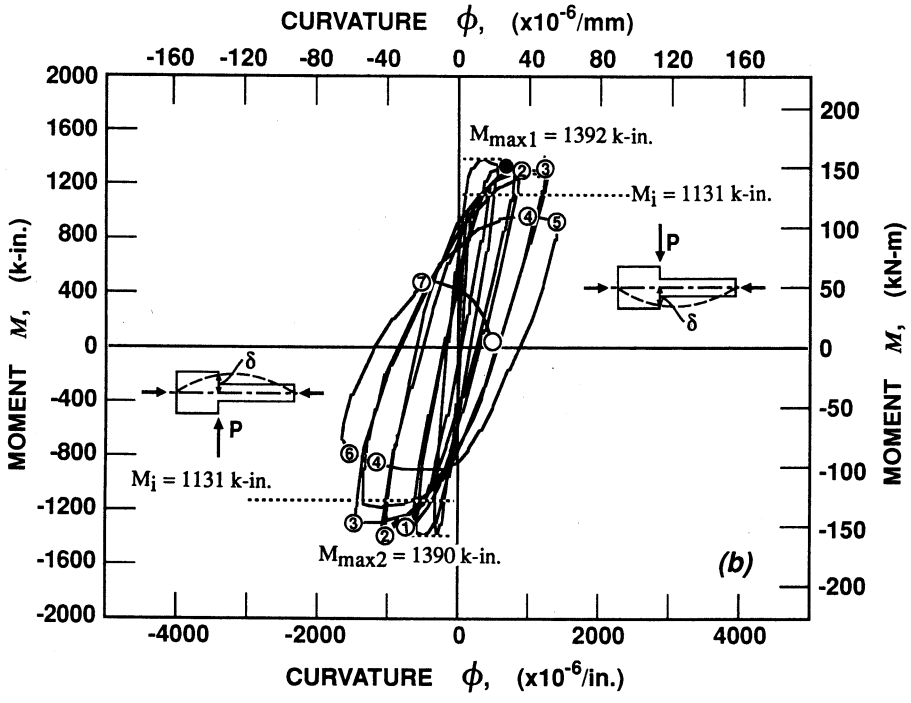

● Spalling of top cover concrete
① Spalling of bottom cover concrete
② Yielding of perimeter tie
③ Yielding of cross-tie
④ Opening of 90° hook
⑤ Buckling of top middle bar
⑥ Buckling of bottom middle bar
⑦ Buckling of additional bars
○ Axial load dropped rapidly

SPECIMEN FS-9

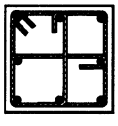

f_c' (ksi)	s (in.)	ρ_s (%)	$\frac{P}{f_c' A_g}$
4.70	3.75	1.68	0.76

Fig. 6—Behavior of Specimen FS-9

mencement of failure. Fracture of buckled bars occurred in Specimens AS-3 and AS-18 and brought about the termination of the test. Failure of these two specimens, which contained the amount of lateral steel in excess of the code requirements, did not result from confinement weakness. The integrity of the core concrete was maintained intact until the fracture of bars occurred. The drift ratio in these columns can be estimated from load-deflection curves shown in Fig. 6

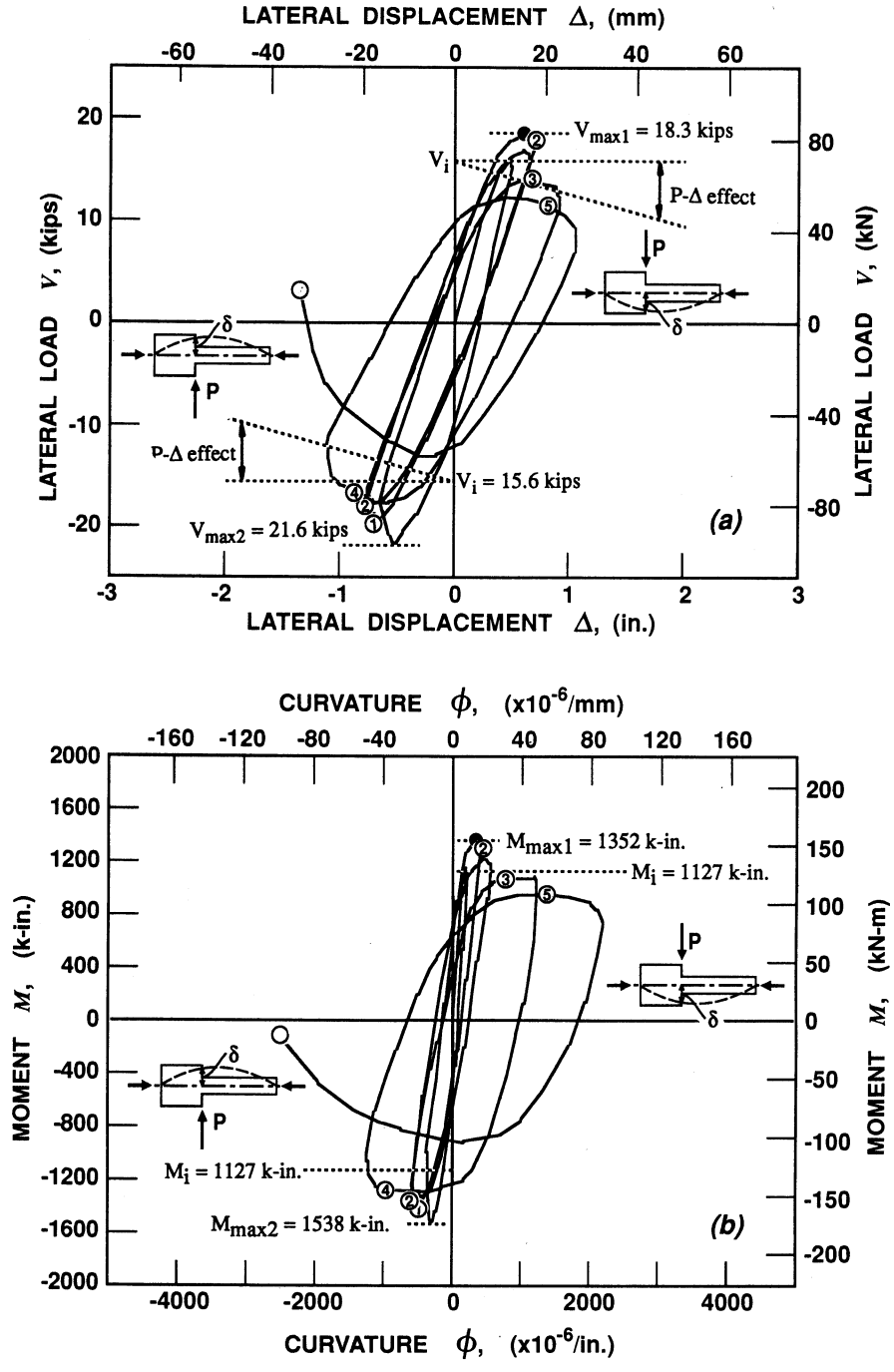

Fig. 7—Behavior of Specimen ES-13

through 11. A 1-in. (25.4-mm) deflection represents a story drift ratio of approximately 1.7 percent if columns are the sole contributor. The maximum deflection of approximately 5.5 percent of column length was experienced by Specimen AS-19, which contained lateral reinforcement a little more than that recommended by the ACI Building Code.[4]

Ductility parameters

Ductility may be defined easily in the case of elasto-plastic behavior. However, in reinforced concrete members lacking such characteristics, there is no universal definition for ductility. Thus, in evaluating the column performance and studying the effects of different variables, ductility and tough-

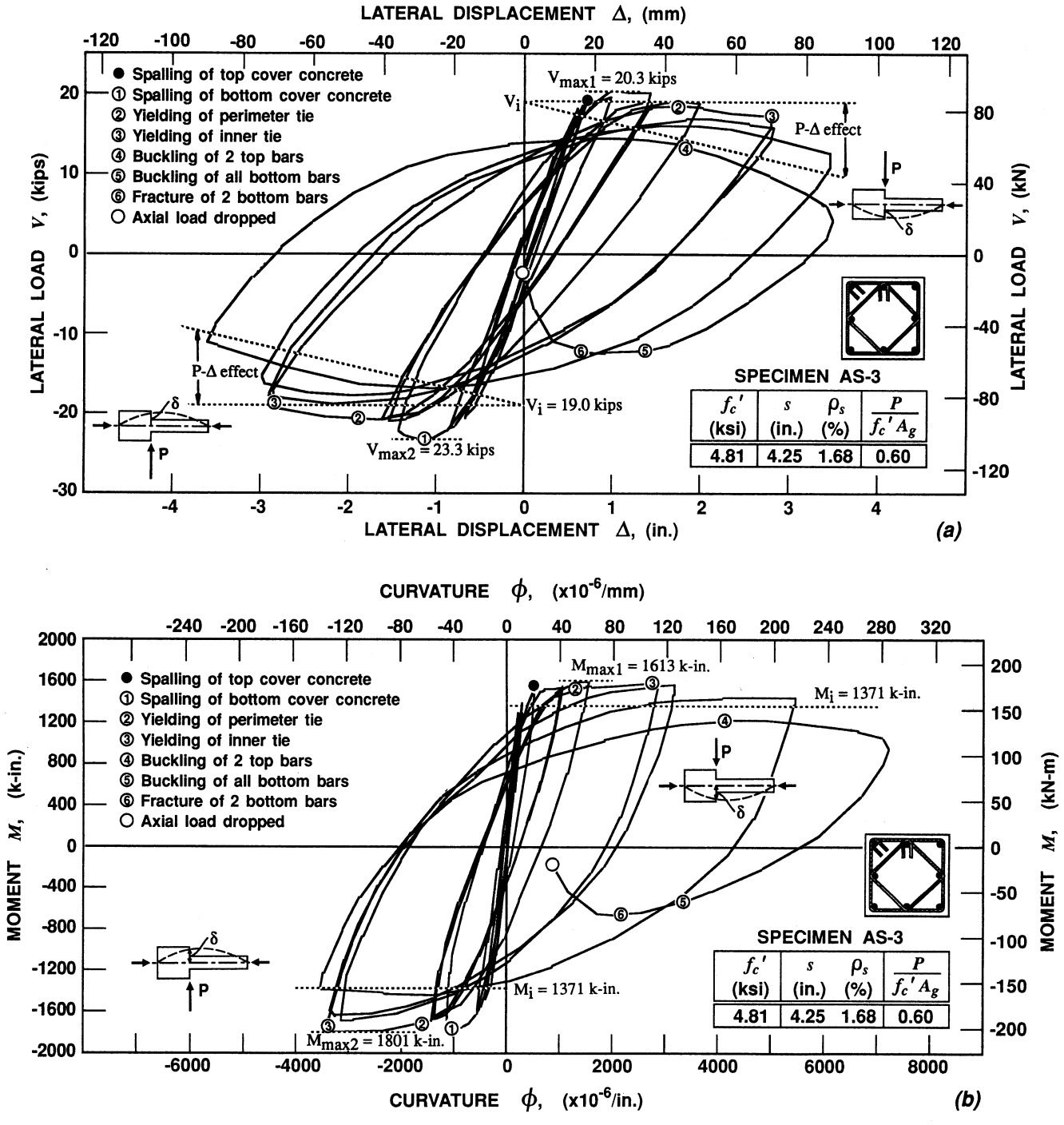

Fig. 8—Behavior of Specimen AS-3

ness are defined using different parameters as given in the following, and are assumed to provide a reasonable basis for consistent evaluation of section and member behavior.

Fig. 12 describes various ductility parameters which include ductility factors μ_ϕ and μ_Δ, cumulative ductility ratio N_ϕ, N_Δ, energy-damage indicator E, and work-damage indicator W. Subscripts t or 80 added to N_ϕ, N_Δ, E, and W indicate the value of each parameter until the end of the test or until the end of the cycle in which the force or the moment is dropped to 80 percent of the maximum value, respectively. All the terms are defined in Fig. 12 except L_f and t, which represent the length of the most damaged region measured from the test and the depth of column section, respectively. Whereas the ductility factor and cumulative ductility ratio represent the extent to which the section or member can deform in the inelastic range, the damage indicators relate to the energy absorbed in the section or the member. All the parameters are nondimensionalized for comparison of different specimens. The work damage indicator is similar to the one proposed by Ehsani and Wight.[8] Table 1 lists the ductility parameters for all the specimens. The curvature ductility factors μ_ϕ are listed for 10 as well as 20 percent drops in the moment capacity.

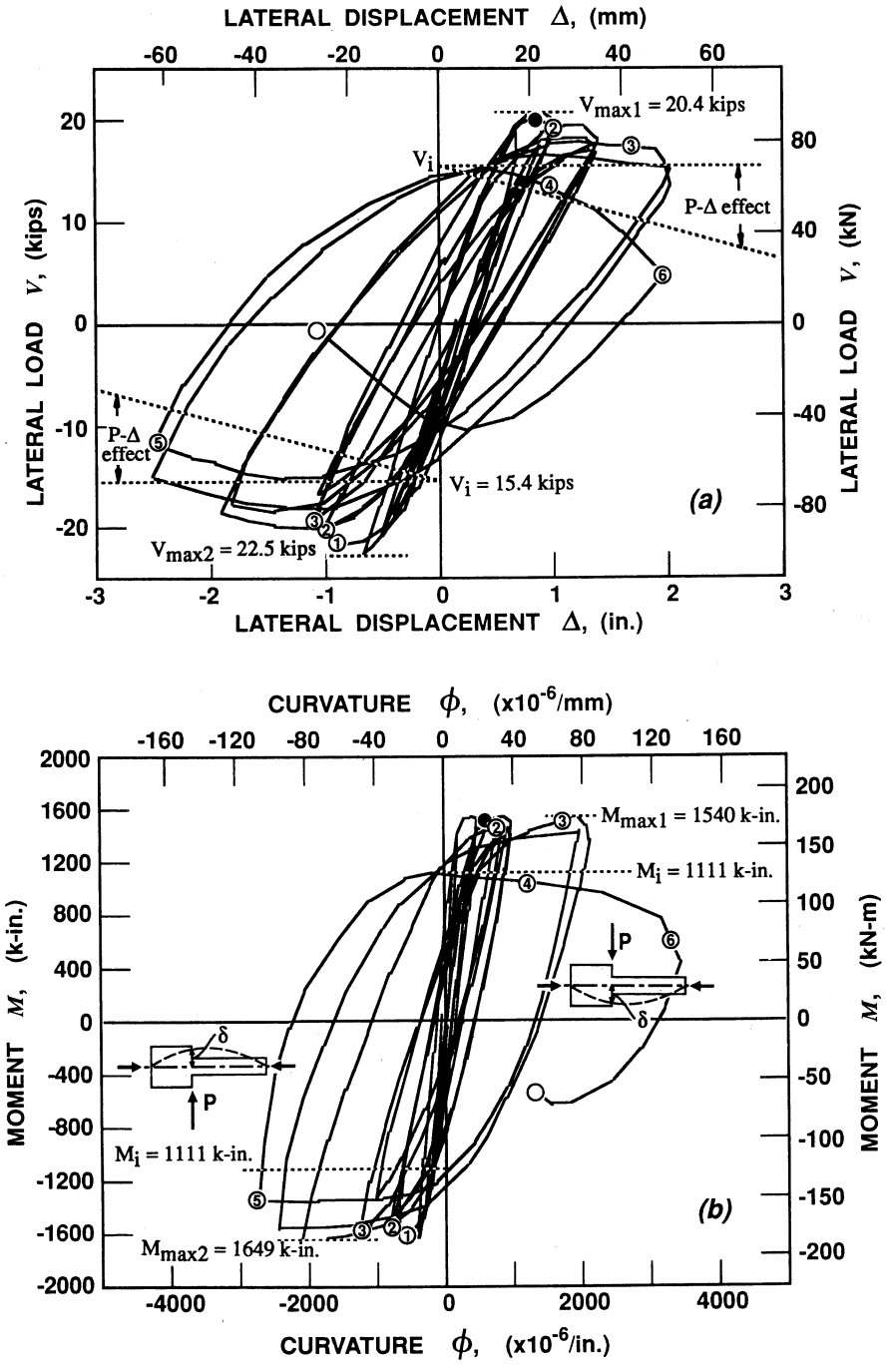

- ● Spalling of top cover concrete
- ① Spalling of bottom cover concrete
- ② Yielding of perimeter tie
- ③ Yielding of inner tie
- ④ Yielding of 2 top bars
- ⑤ Buckling of all bottom bars
- ⑥ Buckling of additional bars
- ○ Axial load dropped rapidly

SPECIMEN AS-17

f_c' (ksi)	s (in.)	ρ_s (%)	$\frac{P}{f_c' A_g}$
4.54	4.25	1.68	0.77

Fig. 9—Behavior of Specimen AS-17

DISCUSSION OF TEST RESULTS

The noticeable differences in the V-Δ and M-ϕ plots among the tested specimens (Fig. 6 through 11) indicate that confinement is affected greatly by different variables. Of primary concern is the section behavior represented by the M-ϕ relationship because, once the column is loaded in the post-elastic range, the deformations concentrate at the plastic hinge positions; hence, further lateral displacement will take place as a result of plastic deformation at the critical section of the column. For ease of comparison between various specimens,

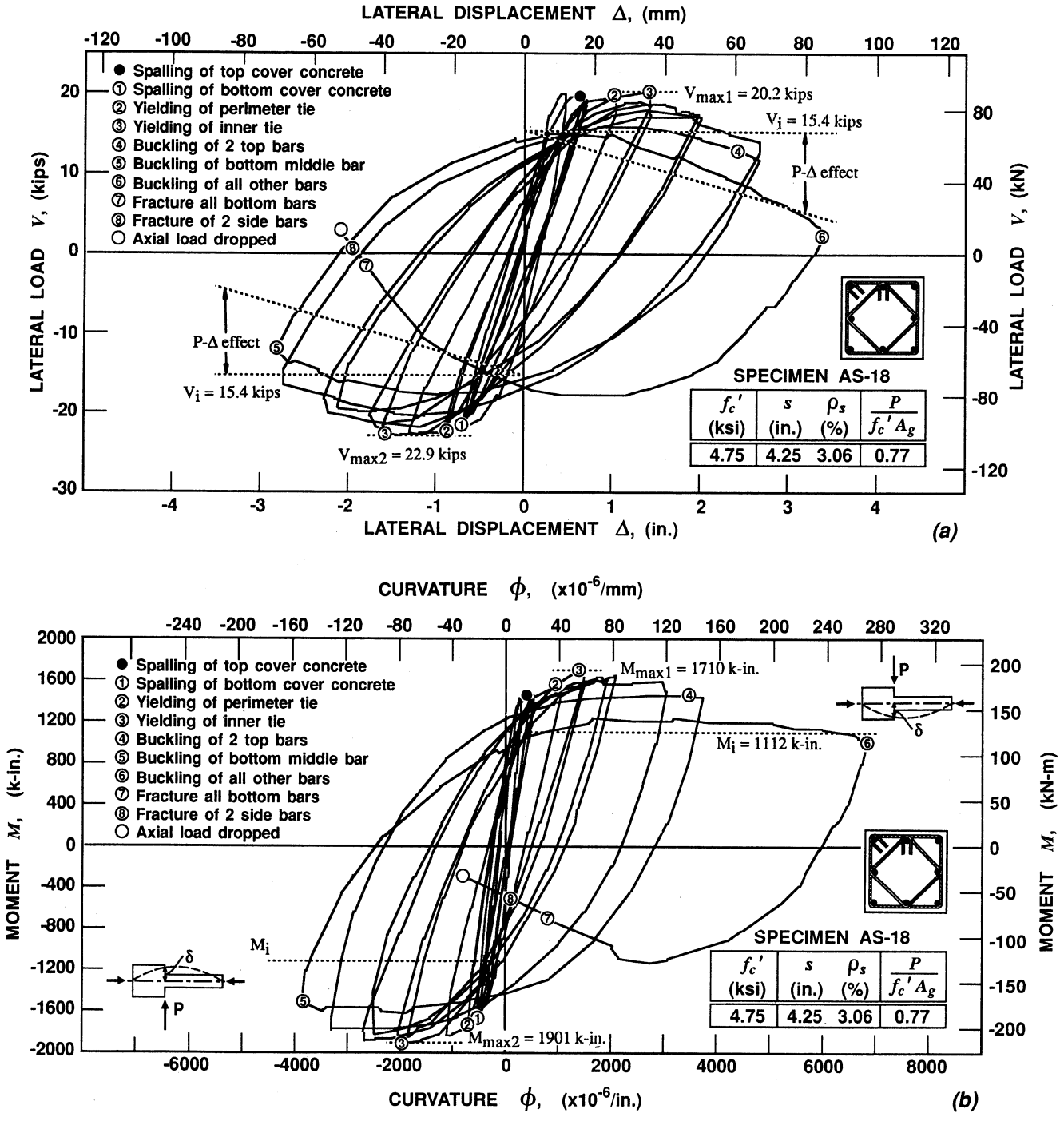

Fig. 10—Behavior of Specimen AS-18

envelope moment-curvature curves are also developed, in which the moment axis is normalized with respect to M_i. Effects of different variables are discussed in the following.

Axial load level

The effect of axial load level on the cyclic behavior of confined concrete is evaluated by comparing the results of the two identical Specimens AS-3 and AS-17 (Fig. 8 and 9) which were tested under axial load levels of $0.6 f_c' A_g$ and $0.77 f_c' A_g$, respectively. Both specimens contained the same amount of lateral steel, which was about 45 percent higher than the ACI Building Code requirements. The normalized M-ϕ envelope curves are compared in Fig. 13. Specimen AS-3 showed more stable hysteresis loops and better energy-dissipation properties than Specimen AS-17. It is evident that an increase in axial load reduces ductility significantly. Section ductility appears to be more sensitive to the level of axial load than member ductility. Increased neutral axis depth under larger axial load and a limited ultimate strain are responsible for the reduced ultimate curvature and ductility.

Introducing Specimen AS-19 at this point raises an important issue. This specimen was tested at a relatively low level of axial load ($P/f_c' A_g = 0.47$) as compared to Specimens AS-3 and AS-17 ($P/f_c' A_g = 0.60$ and 0.77, respectively). The

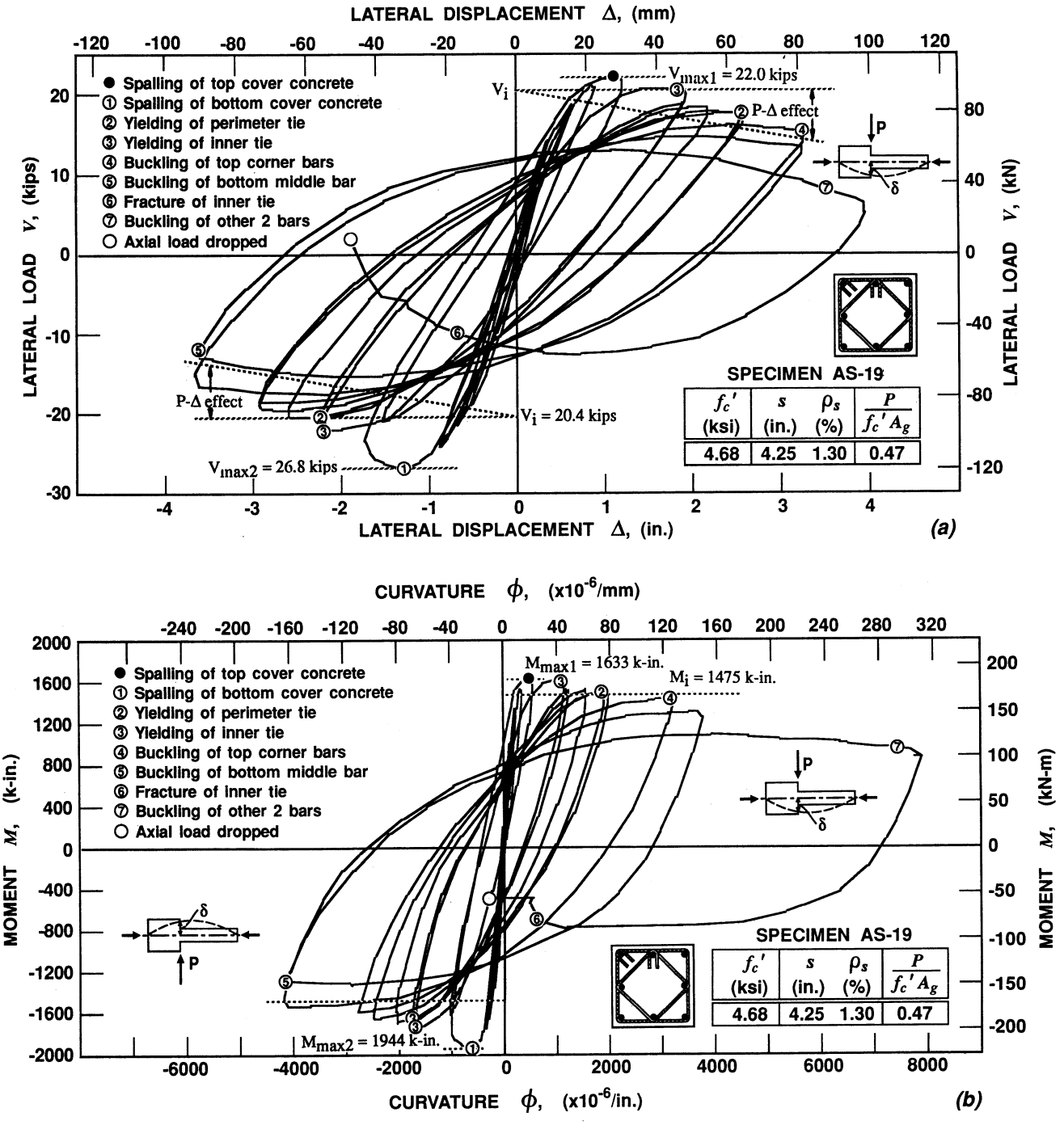

Fig. 11—Behavior of Specimen AS-19

lateral reinforcement ratio ρ_s in Specimen AS-19 was 1.3 percent, which is less than that in Specimens AS-3 and AS-17 (ρ_s = 1.68 percent).

As evident from Fig. 8 and 11 and the ductility parameters in Table 1, Specimens AS-3 and AS-19 behaved very similarly. The adverse effect of the increase in axial load level ($P/f_c'A_g$) from 0.47 to 0.60 is compensated by an increase in lateral reinforcement ratio ρ_s from 1.3 to 1.68 percent. Thus, it can be stated that the code-required steel, as provided approximately in Specimen AS-19, is adequate to supply ductile performance of a column with the steel configuration used, under low to moderate levels of axial load. For lower axial load, the amount of lateral steel can be reduced, and for higher axial load, a larger quantity of tie steel is required to provide comparable ductile performance.

In addition, comparing the behavior of Specimens AS-17 and AS-19 indicates that using an amount of lateral steel about 50 percent more than that required by the code did not provide as ductile a column performance under high axial load as obtained from a specimen containing code-required steel and tested under lower axial load. Note that actual yield stress was used in calculating the code-required amount of tie steel.

Steel configuration

Most North American design codes[4,5] allow the use of Configurations E, F, and A in columns without differentiating be-

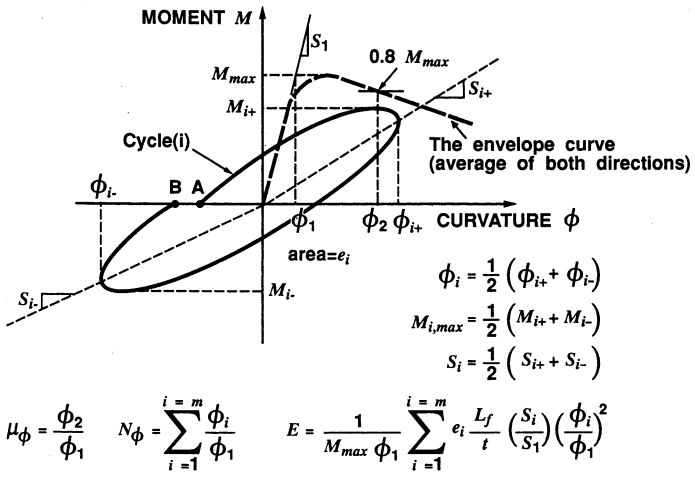

(a) Section Ductility Parameters

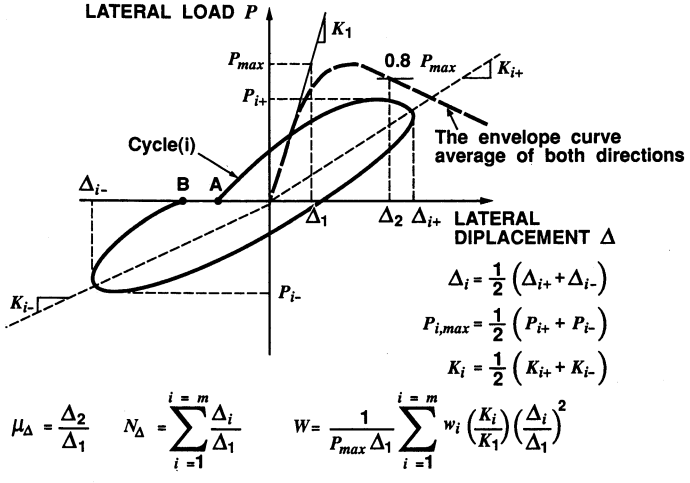

(a) Member Ductility Parameters

Fig. 12—Definitions of ductility parameters

tween the efficiency of confinement in each configuration. To evaluate the effect of this factor, the test results of the three Specimens FS-9, ES-13, and AS-17 can be compared from Fig. 6, 7, and 9. The three specimens had the same amount of lateral and longitudinal steel, similar tie spacing, and were tested under similar levels of axial load (0.76 $f_c'A_g$). Comparisons between the envelope curves of the three specimens are shown in Fig. 14.

The poorest behavior among the three specimens was shown by Specimen ES-13, which endured only five complete load cycles before it lost its ability to maintain the axial load. The measured tie stress in the compression zone when the maximum moment was reached was 56 ksi (386 MPa), which is about 83 percent of the yield stress. After spalling of the cover, the middle bars started to buckle and pushed the ties outward, resulting in a loss of confinement and a rapid deterioration of the specimen. Although the specimen contained more than the code-required amount of lateral steel, a lack of ductility as compared to other specimens is quite obvious. Note that the use of such a steel arrangement is not recommended in the New Zealand code,[6] and was not allowed in the 1956 ACI Building Code.[9]

Unlike Configuration E, the inner ties in Specimen AS-17 were able to provide enough support to the middle longitudinal bars and improve the behavior of the confined concrete core after spalling of the cover. The specimen could undergo 12 complete load cycles before it lost its ability to maintain the axial load, which is more than twice the number of cycles and almost twice the displacement resisted by the companion specimen with E configuration. A very small drop (10 to 15 percent) in the section moment capacity was observed after

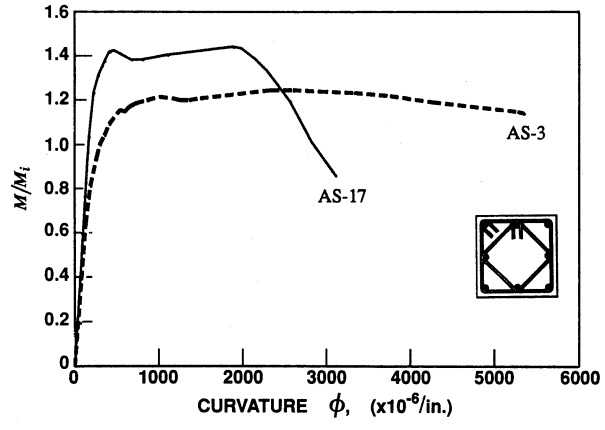

Fig. 13—Effect of axial load

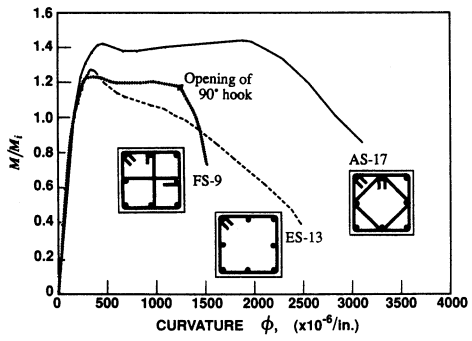

Fig. 14—Effect of steel configuration

spalling of the cover in Specimen AS-17. At that time, the stress in the perimeter tie was about 50 percent of the yield stress [248 MPa (36 ksi)], and the inner tie was stressed to only about 9 ksi (62 MPa). As the test progressed, the tie stress increased and provided additional confining reaction to the concrete core. Thus, the section moment capacity increased further until reaching another peak at a large curvature in Cycle 10. Corresponding to that peak, the tensile stress in the inner ties reached the yield. In the following cycle, the ties yielded again but did not enter the strain-hardening region, and the longitudinal bars started to buckle, indicating the beginning of failure.

Specimen FS-9 behaved quite differently than Specimen

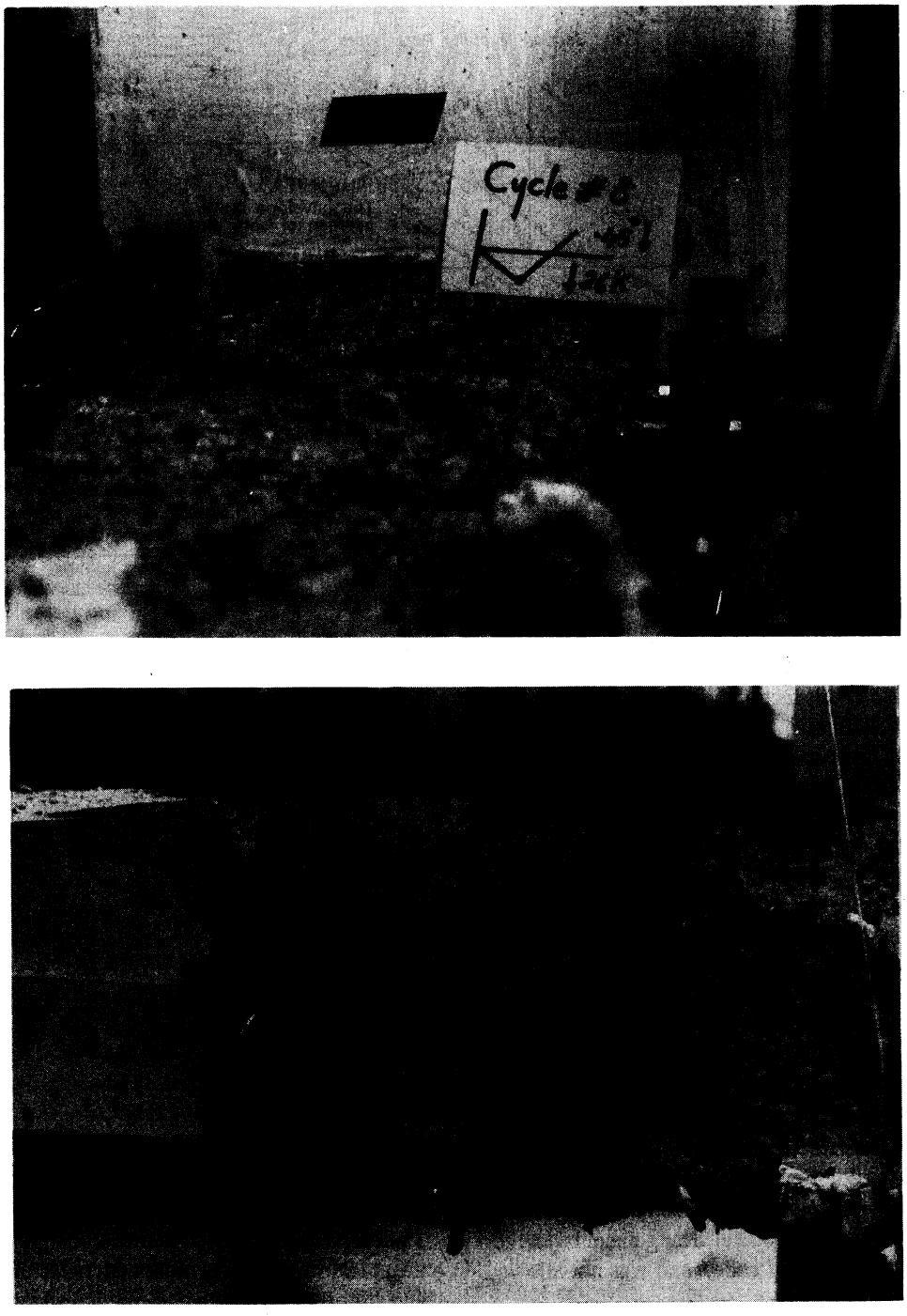

Fig. 15—Gradual opening of 90-deg hook during eighth loading cycle

AS-17, although all the bars in both specimens were supported by tie bends. The specimen behaved in a reasonably ductile and stable manner even after yielding of the perimeter ties in Cycle 4. At that time, the stress in the vertical crosstie was approximately 55 percent of the yield stress. As the stress in this crosstie increased, the 90-deg hook started to open during the eighth cycle, followed by the buckling of the middle bar. As shown in Fig. 14, behavior of the section at this stage deteriorated rapidly as a result of a loss of confinement. Fig. 15 shows the gradual opening of the 90-deg hook at the failed section, which occurred during the last two cycles and caused failure. Sheikh and Yeh[3] observed similar behavior of 90-deg hooks in their tests on specimens under monotonic flexure and high axial load. Some researchers[10,11] have concluded from their tests that the 90-deg hooks performed quite well. Specimens in these studies were tested under relatively low levels of axial load.

During testing of Specimen FS-9, some sidesway was observed during the fifth load cycle. The specimen was unloaded at that point and realigned before testing was resumed. The deformation in the most damaged region in the case of this specimen was more uniformly spread compared to other specimens, possibly as a result of more than one 90-deg hook opening out. This may be the reason for a different correlation between deflection and curvature behavior of this particular specimen compared with other specimens.

Ductility parameters in Table 1 provide some quantitative measure of relatively superior performance of Configuration A. Up to a 20 percent loss in the moment capacity, Specimen AS-17 was able to dissipate more than eight times the energy dissipated by Specimen ES-13, and 2.5 times the energy dissipated by Specimen FS-9. The moment capacities of the failed section as measured by M_{max}/M_i are approximately 1.44, 1.28, and 1.23, respectively, for Specimens AS-17, ES-13, and FS-9.

Amount of lateral steel

Specimens AS-17 and AS-18 were similar in all respects except for the amount of lateral steel. Specimen 17 had almost one-half the amount of the lateral steel than Specimen 18. Both specimens were tested under a high level of axial load ($0.77 f_c' A_g$). In both specimens, the stresses in the outer and inner ties, corresponding to crushing of the cover, were about 50 and 10 percent of the yield stress, respectively. The inner ties in both specimens yielded when the maximum moment was reached.

As seen in Fig. 9, 10, and 16, an increase in the amount of lateral steel significantly improved the behavior of the specimen. The section moment capacity was still increasing after spalling of the cover in Specimen AS-18, indicating an excellent confinement of the concrete core. The degree of enhancement in the moment capacity of the failed section in this specimen is about 62 percent due to confinement, compared with 44 percent in Specimen 17. Under a high axial load level, the confining steel used in Specimen 18, which is about 240 percent of the code requirement, provided ductility factors μ_Δ and μ_ϕ of about 6.7 and 17.5, respectively. Specimen 17, which contained about 150 percent of the code-recommended steel, displayed μ_Δ and μ_ϕ of about 3.8 and 12, respectively.

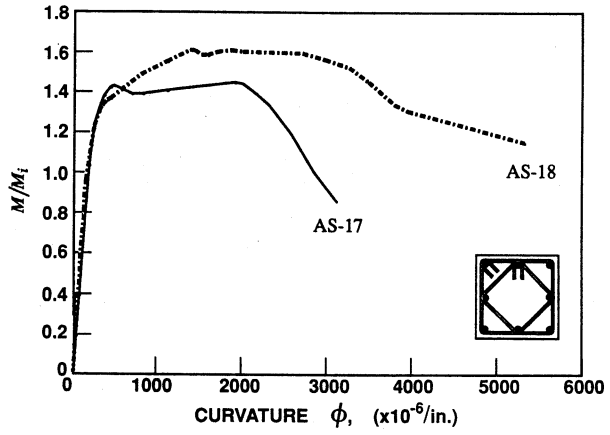

Fig. 16—Effect of amount of lateral steel

As shown in Table 1, other ductility parameters are also significantly higher for Specimen 18 than for Specimen 17.

Stub effect

The section undergoing maximum moment did not fail in any of the specimens. The restraint provided by the stubs strengthened the adjacent critical sections and pushed the failure away from the stub. Fig. 17 shows a typical column failure and sketches of the extensively damaged regions in the six specimens. In all the specimens, the failure initiated at a distance ranging from 9 to 13 in. (225 to 325 mm) away from the stub face and later extended toward the stub. It is believed that restraint from the stub reduced gradually due to the reduced stiffness of the region after the failure was initiated. At the section where the failure initiates, the external restraint from the stub is minimal and the applied moment first exceeded the capacity at that location. It then follows that the moment capacity of that section should correspond approximately to the section capacity in a companion prismatic specimen.

Fig. 18 shows a comparison of the normalized moment-curvature behavior of similar sections in prismatic and nonprismatic stub specimens. Results of prismatic specimens under monotonic flexure and axial load were reported by Sheikh and Yeh.[3] Assuming the validity of the envelope-curve concept, it is obvious that behavior of similar sections in the two companion specimens are similar and that the sections where failure initiated in the stub specimens are mostly free of the restraint from the stubs. In the three stub specimens shown in Fig. 18, the maximum moment at the stub-column interface was approximately 10 percent higher than the moment at failed sections; the moment capacity of the failed sections, in turn, was approximately 25 percent higher than the unconfined moment capacity. Moment at the section where failure initiated was about 5 to 10 percent less than that shown in Fig. 18. Note that the higher moment at the critical sections adjacent to stub did not cause failure. The capacities of these sections are therefore larger than the maximum moment values M_{smax} listed in Table 1 and are unknown. It is believed that the moment enhancement due to stub-restraining effect

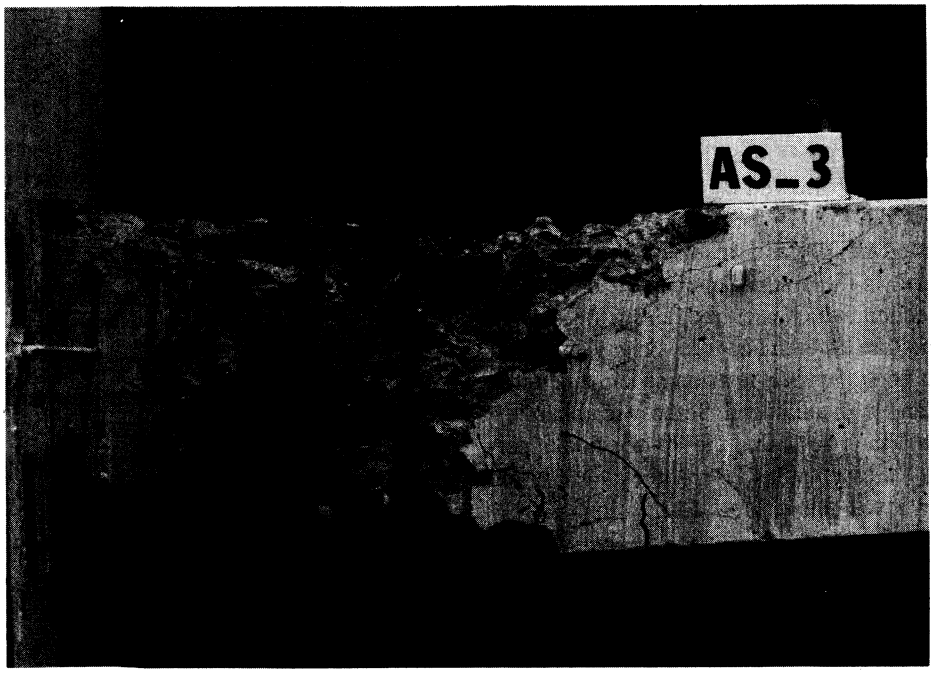

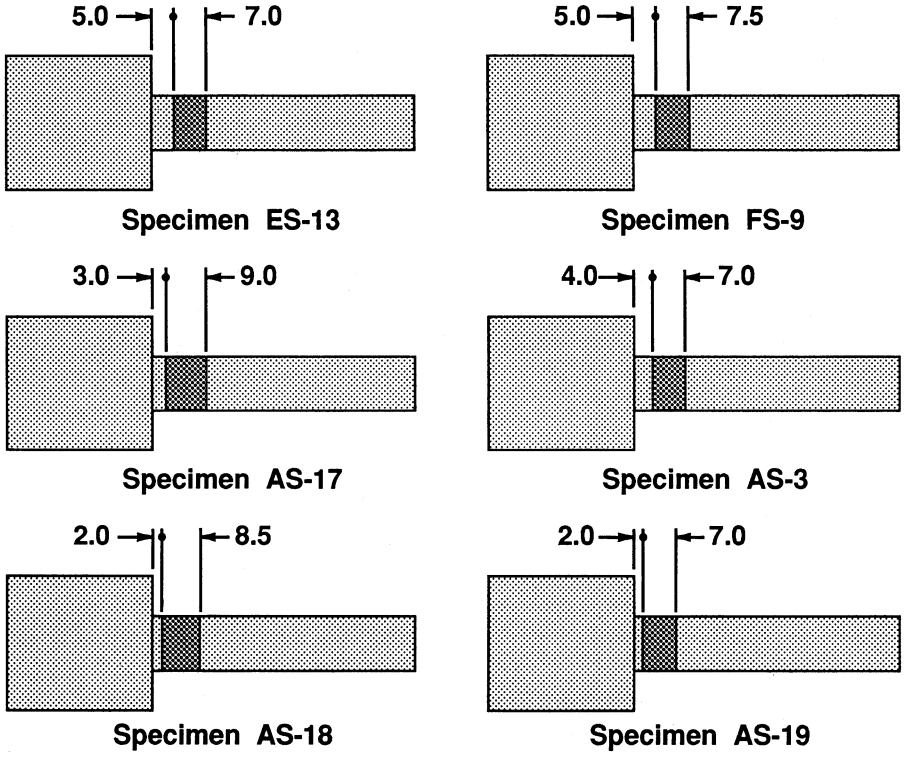

Fig. 17—Extensively damaged regions in specimens

is dependent upon the relative sizes of column and stub. However, the region over which this effect is significant is approximately equal to the column section dimension. For a safe estimate of the design shear force calculated from end moment capacities, appropriately reduced column length should be used.

Concrete compressive strain

The measurements from the LVDTs over about an 8-in. (203-mm) gage length within the failure zone were used to calculate the compressive strain in concrete at various stages of loading. Table 2 lists the strains in concrete at crushing of cover concrete and the maximum strain at the edge of concrete core ε_{max}, which was measured at peak displacement in the last complete cycle of loading. It was felt that ε_{max} is the useful or usable compressive strain for confined concrete and provides a measure of concrete deformability. In all the specimens of Configuration A, the moment carried by the most

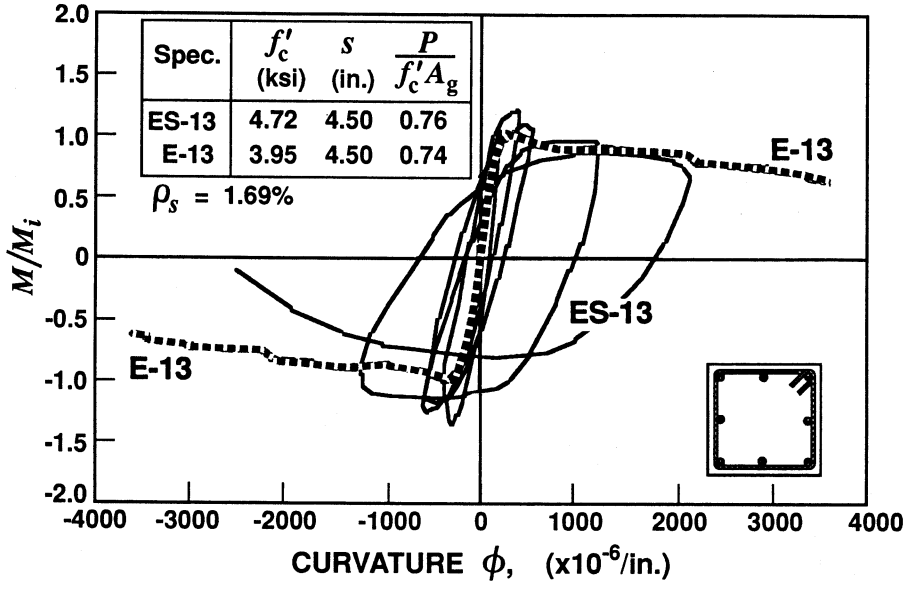

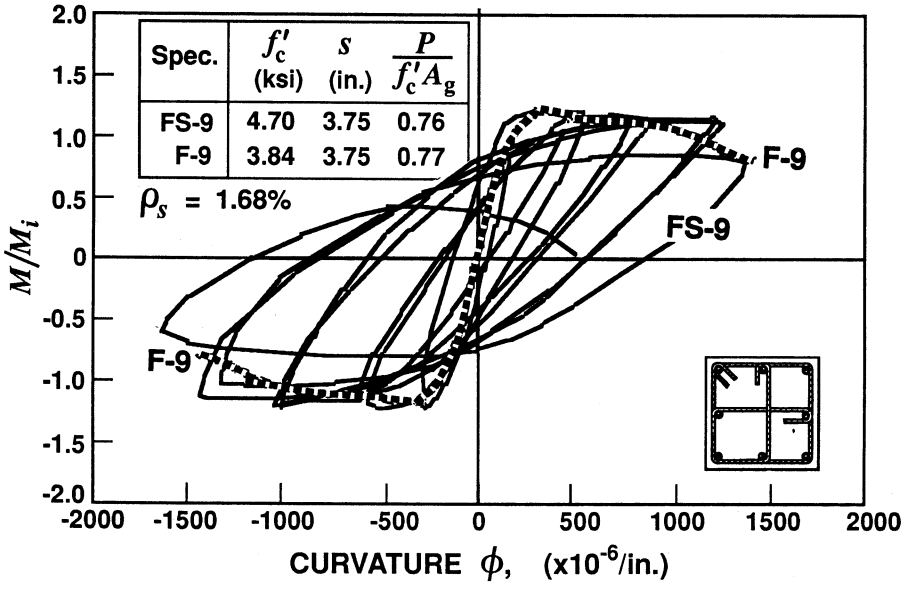

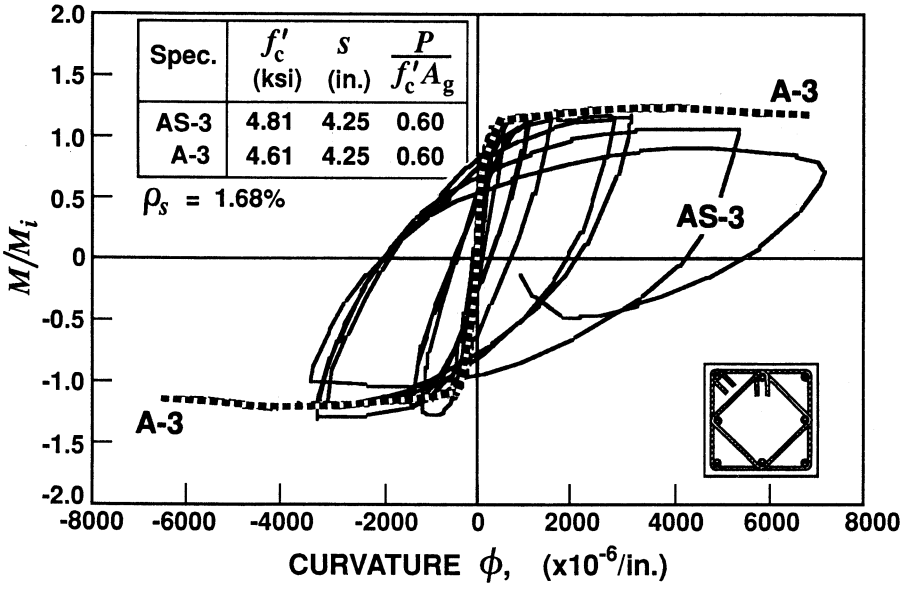

Fig. 18—Effect of stub restraint

Table 2 — Concrete compressive strain and plastic hinge length

Specimen	Experimental strain values		Equivalent plastic hinge length	
	First visible crushing	ε_{max}*	L_p, in.	L_p/h
ES-13	0.0058	0.025	10.2	0.85
FS-9	0.0062	0.037	13.1	1.10
AS-3	0.0045	0.038	11.5	0.96
AS-17	0.0050	0.033	12.6	1.05
AS-18	0.0062	0.042	11.9	0.99
AS-19	0.0063	0.036	13.9	1.16

*Corresponding to the maximum applied displacement in the last complete cycle, as an average of both load directions.

damaged section at this stage was still within about 10 percent of the maximum moment experienced by the section during load excursions.

As seen in Table 2, the crushing strain varied from 0.0045 to 0.0063 with an average value of 0.0057, which is well above the 0.003 that is commonly used. The useful strain ε_{max} varied between 0.025 and 0.042. At this strain, concrete still carried compressive stresses close to its maximum value.

Equivalent plastic hinge length

If equivalent plastic hinge length is defined as the length over which the plastic curvature is assumed to be constant, it can be calculated for a cantilever column from the following equation

$$\Delta_p = \Delta_{max} - \Delta_1 = (\phi_{max} - \phi_1)L_pL \qquad (1)$$

where Δ_1 and ϕ_1 are defined in Fig. 12; L_p = equivalent plastic hinge length and L is the length from column end to the center of the plastic hinge. Using the preceding equation, L_p was calculated for each specimen tested for all the load cycles in which μ_Δ is greater than 4, at least for the last two cycles. For Specimens 9, 13, and 17, L_p was calculated for two cycles, whereas for Specimens 3, 18, and 19, the numbers of cycles over which L_p was averaged were 3, 6, and 4, respectively. The average L_p for each column is listed in Table 2. It appears that L_p is independent of steel configuration, level of axial load, and the amount of lateral reinforcement, and is equal approximately to a section depth of 12 in. (305 mm) in all cases. In fact, the average L_p for six columns is 12.2 in. (310 mm). Obviously, a larger database is required on similarly tested columns before any definite relationship can be established between L_p and different parameters. Note that L_p as calculated includes the effects of yield penetration into the stub and any diagonal tension cracking.

SUMMARY AND CONCLUSIONS

As for specimens under concentric compression and under axial load and monotonic flexure, behavior of columns under axial load and cyclic shear and flexure is also greatly influenced by confinement provided by rectilinear ties.

Steel configuration, including the type of lateral support provided to the longitudinal bars, plays an important role in column performance. The columns with only four corner bars supported by tie bends (Configuration E) performed the worst while Configuration A, in which all eight bars are supported appropriately, performed the best. Unsupported bars buckle prematurely and push the perimeter tie out, resulting in a sudden release of confinement and, hence, failure. Crossties with 90-deg hooks not anchored inside the core (Configuration F) provide good support to the longitudinal bars initially, but at large deformations the hooks open outward, resulting in a sudden column failure, particularly under large axial loads. The column with Configuration A was able to dissipate more than 8 and 2.5 times the energy dissipated by comparable columns with Configurations E and F, respectively.

An increase in the amount of lateral steel results in a significant improvement in strength, ductility, and energy-absorption capacity of columns. Enhancement in ductility and energy-absorption capacity as measured by various parameters appears to be proportional to the increase in lateral steel content; however, the section moment capacity is affected less. In the tests reported here, an increase in the moment capacity in excess of 60 percent was observed due to lateral confinement.

Increased axial load reduces ductility significantly. In comparable columns, the curvature ductility factor reduced by about 45 percent due to an increase in axial load from 0.6 $f_c'A_g$ to 0.77 $f_c'A_g$. This emphasizes the necessity to relate the required amount of lateral steel to the axial load or limit the level of axial load in certain cases when highly ductile performance may be desired.

A heavy stub provides additional confinement to the adjacent section and, in the tests reported here, increased section moment capacity by more than 20 percent. The failure is thus moved to a section away from the stub where the stub-restraining effect is minimal. The design shear should therefore be calculated based on the length between plastic hinges, which may be approximately h to $2h$ smaller than the clear column length, where h is the section depth.

Since the North American design codes do not consider such factors as steel configuration, level of axial load, and presence of stub adjacent to potential plastic hinge regions in the design of confining steel, the columns designed according to code provisions may, under certain circumstances, fail in a brittle manner when subjected to large inelastic deformations. In other situations, code provisions are unnecessarily conservative.

ACKNOWLEDGMENTS

Research reported here was supported by grants from the Natural Sciences and Engineering Research Council of Canada and the National Science Foundation. Laboratory assistance of former graduate students S. Patel and D. Shah is gratefully acknowledged.

CONVERSION FACTORS

1 in. = 25.4 mm
1 psi = 0.006895 MPa
1 ksi = 6.895 MPa

1 kip - in. = 0.113 kN - m
1 kip = 4.448 kN

REFERENCES

1. Sheikh, S. A., and Uzumeri, S. M., "Strength and Ductility of Tied Concrete Columns," *Journal of the Structural Division,* ASCE, V. 106, ST 5, May 1980, pp. 1079-1102.

2. Sheikh, S. A., and Uzumeri, S. M., "Analytical Model for Concrete Confinement in Tied Columns," *Journal of the Structural Division,* ASCE, V. 108, ST 12, Dec. 1982, pp. 2703-2722.

3. Sheikh, S. A., and Yeh, C. C., "Tied Concrete Columns under Axial Load and Flexure," *Journal of the Structural Division,* ASCE, V. 116, No. 10, Oct. 1990, pp. 2780-2801.

4. ACI Committee 318, "Building Code Requirements for Reinforced Concrete and Commentary (ACI 318-89/ACI 318R-89)," American Concrete Institute, Detroit, 1989, 353 pp.

5. "Code for the Design of Concrete Structures for Buildings (CAN3-A23.3-M84)," Canadian Standards Association, Rexdale, 1984, 281 pp.

6. "Code of Practice for the Design of Concrete Structures (NZS 3101:1982)," Standards Association of New Zealand, Wellington, 1982, Part 1, 127 pp.; and Part 2, 156 pp.

7. Khoury, S. S., and Sheikh, S. A., "Behavior of Normal and High Strength Confined Concrete Columns with and without Stubs," *Research Report* No. UHCEE 91-4, Department of Civil and Environmental Engineering, University of Houston, Dec. 1991, 345 pp.

8. Ehsani, M. R., and Wight, J. K., "Confinement Steel Requirements for Connections in Ductile Frames," *Journal of the Structural Division,* ASCE, V. 116, ST 3, Mar. 1990, pp. 751-767.

9. ACI Committee 318, "Building Code Requirements for Reinforced Concrete (ACI 318-56)," American Concrete Institute, Detroit, 1956, 75 pp.

10. Rabbat, B. G.; Daniel, J. L.; Weinmann, T. L.; and Hanson, N. W., "Seismic Behavior of Lightweight and Normal Weight Concrete Columns," ACI JOURNAL, *Proceedings* V. 83, No. 1, Jan.-Feb. 1986, pp. 69-79.

11. Saatcioglu, M., and Ozcebe, G., "Response of Reinforced Concrete Columns to Simulated Seismic Loading," *ACI Structural Journal,* V. 86, No. 1, Nov.-Dec. 1989, pp. 3-12.